

Comment on “Current routes in hydrogenated microcrystalline silicon”

A. Vetushka,* A. Fejfar, M. Ledinský, B. Rezek, J. Stuchlík, and J. Kočka

Institute of Physics, Academy of Sciences of the Czech Republic v.v.i., Cukrovarnická 10, 162 00 Prague 6, Czech Republic

(Received 3 June 2009; published 4 June 2010)

We show that local currents observed by the conductive atomic force microscopy (C-AFM) of silicon thin films measured in ambient atmosphere are generally limited by surface oxide, either native or created by the measurement itself in a process of local anodic oxidation. The tip-induced oxidation changes character of the local current maps, either in repeated scans or even in the first scan of a pristine surface. In particular, the preoxidation of the neighboring scan lines leads to the appearance of grain edges as conductive rings, previously interpreted as an evidence of the main transport route at the grain boundaries in microcrystalline silicon. We also show that stripping of the surface oxide by HF etch restores the local currents to the values corresponding to C-AFM done in ultra-high-vacuum on *in situ* deposited samples.

DOI: [10.1103/PhysRevB.81.237301](https://doi.org/10.1103/PhysRevB.81.237301)

PACS number(s): 73.50.-h, 68.37.Ps, 81.65.-b, 72.20.-i

Hydrogenated microcrystalline silicon ($\mu\text{c-Si:H}$), a material important especially for thin film solar cells, has complicated microstructure consisting of columnar grains surrounded by disordered tissue and/or amorphous phase.¹ The variability of structure and resulting electronic transport properties has led to a controversy over the dominant charge transport mechanism^{2,3} and, in particular, over the location of the dominant transport route.⁴ The capability of scanning probe microscopy (SPM) to measure local currents with nanometer resolution offers a chance to look for the transport route directly by identifying more conductive parts of the $\mu\text{c-Si:H}$ samples.⁵⁻⁷ The conductive atomic force microscopy (C-AFM) (Ref. 5) was also used in a paper⁴ in which Azulay *et al.* observed higher local currents at the edges of isolated grains. They concluded that the conductivity through (via) a percolating network of a disordered tissue surrounding the columnar grains dominates over other possible routes, as illustrated by their Fig. 1(a).

First of all, we have to mention that Azulay *et al.*⁴ claimed that there was a “discrepancy between our macroscopic and microscopic data” (see Refs. 5 and 27 in Ref. 4), which they tried to explain by oxygen doping of the disordered tissue. However, there is no discrepancy between our results. We have never said that in macroscopic measurements transport via disordered grain boundary tissue dominates. Our model of transport,^{1,3,8} which is in agreement with both our macroscopic and microscopic data (and actually corresponds to the “full-line” transport path from Fig. 1a of Ref. 4), is based on the idea that whenever the “large grain boundaries” (LGBs) are formed, the bandlike transport is blocked by these resistive LGB and another path, via localized tail states *within* the grains and through (not along) thin blocking tissue prevails.

Moreover, our samples for microscopic and macroscopic measurements are usually prepared in the same run, at the same vacuum level; their oxygen content is identical and as low as state-of-the-art thin film Si of the other authors. Eventual aging (oxygen intake), possible for some highly crystalline and porous $\mu\text{c-Si:H}$, is again the same for macroscopic and microscopic measurements when C-AFM is done in air. We have used UHV setup (mentioned in Ref. 4 to support the claim of different oxygen content in our samples) just for our first C-AFM measurements^{5,7} to prevent native oxide formation. The samples have been prepared in standard plasma

enhanced chemical-vapor deposition (PECVD) chamber and transferred *in situ* to C-AFM UHV system.

The fact that conductive grain boundaries are in direct conflict with our model stimulated our interest. We tried to verify the results in Ref. 4, suspecting at first that the higher conductivity at the grain boundaries resulted from a geometrical effect of the tip with worn metallic coating.⁷ On the way we have discovered a completely different origin of the higher conductivity at the grain boundaries, namely, the influence of surface oxidation induced by the tip when the sample is positively biased. This effect, denoted as local anodic oxidation (LAO), is well known and is often used for

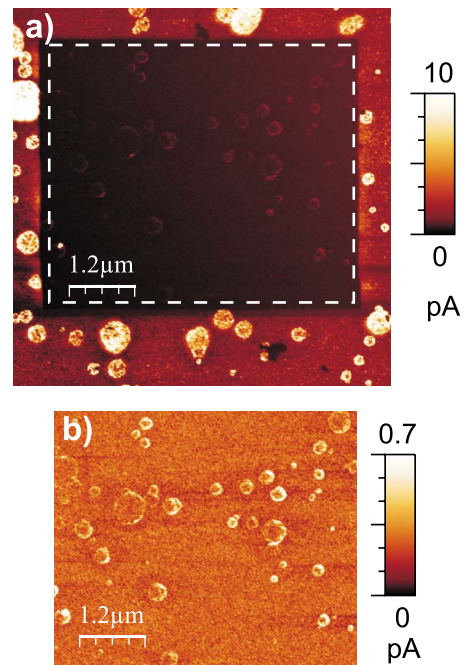


FIG. 1. (Color online) Memory effect in the local current image of $\mu\text{c-Si:H}$ thin film. The $6 \times 6 \mu\text{m}^2$ scan shown in (a) was measured by C-AFM at -5 V bias applied to the sample after the previous $+10 \text{ V}$ scan of the central area $5 \times 4.5 \mu\text{m}^2$. The previously scanned (dark) area is not only less conductive, but it also shows a different character as seen in (b) where it is plotted again with adjusted color scale. The grains now appear more conductive at the edges.

SPM lithography.⁹ It was also considered as one of the reasons for so-called memory effect, i.e., lowering of the local currents observed by C-AFM in the second scan of the same area of the Si surface.¹⁰⁻¹² Here we present a surprising effect of LAO on C-AFM, namely, that the tip induced oxidation can make the grain boundaries appear more conducting even in the very first scan of a pristine surface.

We have used a thin film of $\mu\text{c-Si:H}$ grown on polished crystalline Si wafer (with 0.1 nm rms roughness) by PECVD in a mixture of silane (SiH_4) and hydrogen at the following conditions: discharge frequency 13.56 MHz, dilution ratio of the gas flows $r_H = [\text{H}_2]/[\text{SiH}_4] = 28$, pressure 70 Pa and substrate temperature 250 °C. The conditions were close to the boundary between the amorphous and microcrystalline growth, resulting in a film consisting of relatively few large conical microcrystalline grains surrounded by a smooth amorphous surface, similar as in our previous works^{5,13} and also to the sample used in Ref. 4. The film thickness of 1.1 μm was determined by stylus method (Tencor AlphaStep 100) and the surface crystallinity $17 \pm 2\%$ was determined by AFM.¹⁴

The samples were measured by Veeco Dimension 3100 AFM equipped with the extended TUNA (Tunneling AFM) module for the current detection in the pA range. All AFM results reported below were performed in contact mode using the Cr/Pt coated Si cantilevers (BudgetSensors ContE) with resonant frequency around 13 kHz and force constant 0.2 N/m. We used fresh cantilevers to avoid artifacts due to the conductive layer abrasion.^{7,15} Local current flowing through the grounded cantilever was induced by a dc bias applied to the underlying silicon substrate. The set point of the AFM scan corresponded to the applied normal force around 25 nN and minimal possible scanning speed was used (mostly 500 nm/s). All C-AFM measurements were performed at 25 °C and approx. 30% humidity of the ambient air. Results of the AFM measurements were processed with WSXM software.¹⁶

The results shown in Fig. 1 illustrate the memory effect in ambient C-AFM. The sample was first scanned in a smaller area with a high oxidizing voltage (+10 V), same as in Ref. 4. Then, the current map in Fig. 1(a) was recorded across a bigger area with nonoxidizing voltage of -5 V. The previously scanned area appears dark as the current values were decreased by about one order of magnitude. The same area is rendered in Fig. 1(b) in a finer current scale to visualize the details. It can be seen that the oxidation led not only to overall lower currents but also to a change in features in the current image. The current lowering is more pronounced on the grains than at the grain edges and so the edges appear brighter than the grain interiors. As a result, the grain edges in the oxidized image form rings of relatively higher conductivity.

We have verified that the surface scanned with a high oxidizing voltage underwent topographical changes expected after local anodic oxidation. We have indeed observed approximately 1 nm high surface step at the edge of the area scanned at +10 V. Note that this height does not correspond to the full oxide thickness as there was already some native oxide on the surface and LAO leads to the oxide growth also into the sample interior.⁹ The oxide growth induced by the AFM tip proceeds also laterally and the Fig. 2 shows the

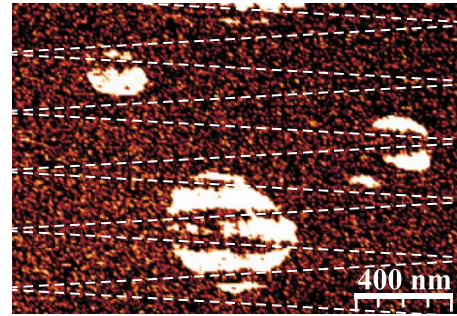


FIG. 2. (Color online) Local current map measured at nonoxidizing -2.5 V bias after the previous zigzag scan (along the path marked by the white dashed line) at +10 V sample bias. The dark (less conductive) lines across the bright (more conductive) grains illustrate the width of the oxidized lines.

result of another experiment designed to find the width of the oxide line. The sample was oxidized in a zigzag pattern (along the path marked by the dashed line in Fig. 2) at +10 V and then imaged as the local current map at -2.5 V. It can be seen that the scanning tip at oxidizing bias leaves behind an oxide line which influenced the local current within approximately 50 nm wide band, in agreement with the minimal line widths in LAO based lithography.⁹

Thus the oxidized line is several times wider than the separation of the individual lines in the typical AFM scans: commonly used 256 lines per image means scan lines are separated by 8 nm for a 2 μm wide field of view. Therefore at oxidizing conditions only the first line actually scans the pristine surface and all subsequent neighboring lines record the local current values on already locally oxidized surface.

Consequently, the neighboring line preoxidation can lead to formation of the conductive rings already in the very first scan of the sample, as shown in Fig. 3. In this case the expected width of the oxidized line (50 nm) is about ten times bigger than the 5 nm separation of the scan lines in Fig. 3. Therefore, before a value in the local current map is recorded, the same point was already oxidized by approximately ten passages of the AFM tip in the previous line scans. The local current image is similar to the image in Fig. 1(b), showing similar current scale and again the conductive rings at the grain edges. When the current map is recorded using nonoxidizing voltage, there is no difference in the character of the local current recorded at the grain edges or in the interior of the grains, similar as in Ref. 5.

As far as we know, the conditions of the scan presented in

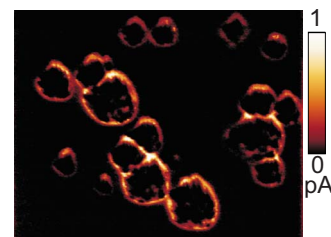


FIG. 3. (Color online) Local conductivity map resulting from C-AFM in the first scan of a pristine area of the sample at voltage +10 V applied to the substrate. Rings with relatively higher conductivity at the $\mu\text{c-Si}$ grain edges are observed.

Fig. 3 were identical to the conditions used in Ref. 4, so we conclude that even in their case the conductive rings were actually an artifact resulting from the tip induced surface oxidation. This is a surface effect for which the oxygen content within the sample is only secondary, offering a simpler explanation of the observed facts than the effect of possible oxygen doping proposed in Ref. 4.

Finally, we want to comment results by current image tunneling spectroscopy (CITS) from Fig. 4 of Ref. 4, which were used to support conductive rings around the grains as detected by C-AFM. First of all, to our best knowledge the samples have been transferred through air. Due to strong sensitivity of the STM to the surface states, lot of things could lead to the observed current traces. Second, the support is weak because the CITS measurements have not been done on the same, low crystallinity ($x=0.2$) sample as C-AFM, but on a highly crystalline ($x=1$) sample with very different properties. Last, the CITS current image in Fig. 4 of Ref. 4 shows enhanced current only on one side of the column while the opposite side of the column appears dark, i.e., less conductive. Note that CITS keeps the tip at certain distance from the surface using tunneling current feedback at one voltage and records the current image at higher voltage at the same distance. Thus this effect most probably reflects the different feedback reaction dependent on the scan direction on the relatively rough (15 nm range) surface of the sample. This effect may be even further enhanced by the increase in voltage due to a nonlinear character of local I - V characteristics.⁷ We have also performed the CITS experiments ourselves (in UHV using *in situ* prepared sample to avoid any oxidation), but the results were inconclusive, just as in the Ref. 4.

The hindered anodic oxidation at the grain edges in ambient C-AFM may arise by a number of different mechanisms. It can be attributed to different geometry of the tip-sample contact at the grain edges to the decline in oxidation rate due to build up of space charge¹⁷ or a higher resistance of the boundary between the grain and surrounding amorphous tissue. In particular, the voltage drop due to the higher boundary resistance would decrease the field assisting the migration of ions necessary for the anodic oxidation and

hence lead to the oxide layer being thinner in the vicinity of the GB. In that case, the conductive rings at the grain edges in oxidized state would actually support the notion of less conductive grain boundaries in μ c-Si:H, as presented in our model of transport in μ c-Si:H (Ref. 8) assuming the lower conductivity of the LGB resulting from the band gap increased by hydrogen and oxygen alloying and leading to the presence of transport barriers.

The oxidation artifacts in μ c-Si:H local current maps can be avoided by not using high positive sample voltages. Furthermore we have successfully tested a simple procedure for removing the oxide from the surface of the silicon films: samples were put into 10% water solution of HF for a few seconds, rinsed by de-ionized water and blown dry by an air jet. This procedure restored the local current values and features to comparable to those measured by C-AFM in UHV on *in situ* prepared samples.⁵⁻⁷ Hence this procedure can be easily used to verify C-AFM results even on aged samples.

To conclude, we have demonstrated how the local anodic oxidation leads to a surprising artifact of the conductive rings at the grain boundaries (see Figs. 1 and 3). The neighboring line preoxidation leads to the appearance of the same effect even in the very first scan of a pristine surface. The observed apparent higher conductivity at the grain edges reflects a state of the surface of the sample and it cannot be used for arguing about the transport route within the material itself. Finally, the artifacts due to neighboring lines may need to be considered not only for silicon thin films¹⁵ but also when C-AFM is used to study other heterostructural materials or nanostructures, e.g., polycrystalline films,¹⁸ bulk organic heterojunctions,¹⁹ nanocomposites,²⁰⁻²² diamond surface structures,²³ semiconductor nanocrystals,^{24,25} or quantum dots.²⁶

This work was supported by the Ministry of Education, Youth and Sports of the Czech Republic through Institutional Research Plan AV0Z 10100521 and projects LC510 and LC06040, by the Grant Agency of the Academy of Sciences of the Czech Republic through projects KAN400100701 and IAA100100902 and by the European Commission through the PolySiMode project, FP7 Grant Agreement No. 240826.

*vetushka@fzu.cz

¹J. Kočka, A. Fejfar, H. Stuchlíková, J. Stuchlík, P. Fojtík, T. Mates, B. Rezek, K. Luterová, V. Švrček, and I. Pelant, *Sol. Energy Mater. Sol. Cells* **78**, 493 (2003).

²I. Balberg, Y. Dover, R. Naides, J. Conde, and V. Chu, *Phys. Rev. B* **69**, 035203 (2004).

³J. Kočka, A. Vetushka, and A. Fejfar, *Philos. Mag.* **89**, 2557 (2009).

⁴D. Azulay, I. Balberg, V. Chu, J. P. Conde, and O. Millo, *Phys. Rev. B* **71**, 113304 (2005).

⁵B. Rezek, J. Stuchlík, A. Fejfar, and J. Kočka, *Appl. Phys. Lett.* **74**, 1475 (1999).

⁶C. Ross, J. Herion, and H. Wagner, *J. Non-Cryst. Solids* **266-269**, 69 (2000).

⁷B. Rezek, J. Stuchlík, A. Fejfar, and J. Kočka, *J. Appl. Phys.* **92**, 587 (2002).

⁸J. Kočka, A. Fejfar, P. Fojtík, K. Luterová, I. Pelant, B. Rezek, H. Stuchlíková, J. Stuchlík, and V. Švrček, *Sol. Energy Mater. Sol. Cells* **66**, 61 (2001).

⁹D. Stiévenard and B. Legrand, *Prog. Surf. Sci.* **81**, 112 (2006).

¹⁰J. P. Kleider, C. Longeaud, R. Brüggemann, and F. Houzé, *Thin Solid Films* **383**, 57 (2001).

¹¹B. Rezek, T. Mates, E. Šípek, J. Stuchlík, A. Fejfar, and J. Kočka, *J. Non-Cryst. Solids* **299-302**, 360 (2002).

¹²B. Rezek, T. Mates, J. Stuchlík, J. Kočka, and A. Stemmer, *Appl. Phys. Lett.* **83**, 1764 (2003).

¹³T. Mates, P. Bronsveld, A. Fejfar, B. Rezek, J. Kočka, J. Rath, and R. Schropp, *J. Non-Cryst. Solids* **352**, 1011 (2006).

- ¹⁴M. Ledinský, A. Vetushka, J. Stuchlík, T. Mates, A. Fejfar, J. Kočka, and J. Štěpánek, *J. Non-Cryst. Solids* **354**, 2253 (2008).
- ¹⁵D. Cavalcoli, M. Rossi, A. Tomasi, and A. Cavallini, *Nanotechnology* **20**, 045702 (2009).
- ¹⁶I. Horcas, R. Fernández, J. Gómez-Rodríguez, and J. Colchero, *Rev. Sci. Instrum.* **78**, 013705 (2007).
- ¹⁷J. A. Dagata, F. Perez-Murano, C. Martin, H. Kuramochi, and H. Yokoyama, *J. Appl. Phys.* **96**, 2386 (2004).
- ¹⁸I. Visoly-Fisher, S. Cohen, K. Gartsman, A. Ruzin, and D. Cahen, *Adv. Funct. Mater.* **16**, 649 (2006).
- ¹⁹J. Čermák, B. Rezek, V. Cimrová, D. Výprachtický, M. Ledinský, T. Mates, A. Fejfar, and J. Kočka, *Phys. Status Solidi (RRL)* **1**, 193 (2007).
- ²⁰A. K. Mann, D. Varandani, B. R. Mehta, and L. K. Malhotra, *J. Appl. Phys.* **101**, 084304 (2007).
- ²¹A. Alexeev and J. Loos, *Org. Electron.* **9**, 149 (2008).
- ²²A. Trionfi, D. A. Scrymgeour, J. W. P. Hsu, M. J. Arlen, D. Tomlin, J. D. Jacobs, D. H. Wang, L.-S. Tan, and R. A. Vaia, *J. Appl. Phys.* **104**, 083708 (2008).
- ²³F. Houzé, J. Alvarez, J. Kleider, P. Bergonzo, E. Snidero, and D. Tromson, *Diamond Relat. Mater.* **15**, 618 (2006).
- ²⁴E. Nahum, Y. Ebenstein, A. Aharoni, T. Mokari, U. Banin, N. Shimoni, and O. Millo, *Nano Lett.* **4**, 103 (2004).
- ²⁵H.-C. Chung, W.-H. Chu, and C.-P. Liu, *Appl. Phys. Lett.* **89**, 082105 (2006).
- ²⁶R. Wu, F. H. Li, Z. Jiang, and X. J. Yang, *Nanotechnology* **17**, 5111 (2006).